Investigating aperture diameter and total falling time of a bucket in a variable mass Atwood machine

1 Introduction

Throughout the IB course, we only analyzed simple systems whose masses remain constant over time. Although in many exam questions, systems of variable masses are implicitly introduced (e.g. cart that moves in rain with water filling at a certain rate). I wondered whether there are some classical systems that I could modify that would produce some interesting results. One such system is the Atwood machine: being the classical demonstration for constant acceleration of constant mass system, I was curious about how its behaviors will change if I made its mass vary over time. Knowing that a system that is losing mass over time is very similar to that of the commonly explored "Rocket problem" in undergraduate textbooks, I wanted to investigate how the theory and concepts change if the variable mass Atwood machine is gaining mass during its motion. This leads to the aim of this paper: How does the diameter of a sand leaking funnel affect the total falling time of a gaining mass Atwood system?

2 Background Information

In classical mechanics, the Atwood machine is usually used to illustrate Newton's laws of motions and the concept of forces. The Atwood machine can be described in Figure 1 (Byjus),

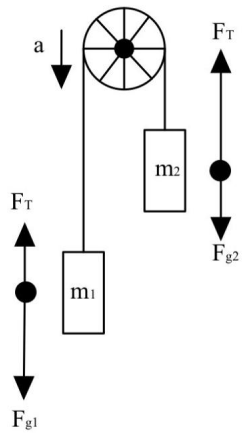

Figure 1: An Atwood machine consisting of two masses(m_1 and m_2) connected via a massless string and a pulley in between.

The Atwood machine consists of two masses attached to a string that is routed over a pulley. An ideal Atwood machine assumes that the string is massless and is not stretchable; and the pulley is frictionless. There are two scenarios associated with the Atwood machine: one is when the two masses are equal, $m_1 = m_2$, in which case, there is no acceleration. In the second case, where one of the masses is greater, there is a net acceleration to the side that has a greater mass.

3 The Experiment

The major modification made to the traditional Atwood machine was the funnel system that consists of sand inside it that would constantly feed sand into the system. This modification can be seen in Figure 2:

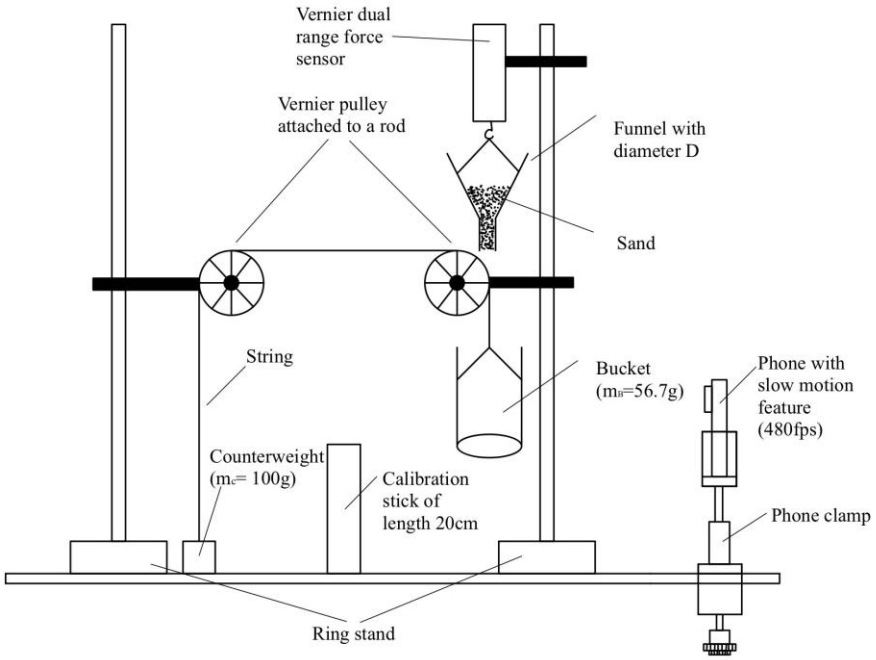

Figure 2: Experimental setup of a variable mass Atwood machine

As shown in Figure 2, two pulleys on the ends of $\frac{1}{2}$-inch diameter rods were clamped to a ring stand using a swivel clamp holder. This ensured that the two pulleys are of approximately the same height. Two masses were connected on the ends of the pulleys through a string: one was a counterweight of mass (m_c=100g) and the other was a bucket of mass (m_B=56.7g). It was also measured that the bucket was of a height h_0=43cm above the table. A vernier dual force sensor was clamped at the top of the ring stand using a swivel clamp holder, with a funnel of diameter D attached to its hook. The vernier dual force sensor is also connected to the computer through a LAB Quest Mini to measure the change in the weight of the funnel over time. The funnel was loaded with approximately 200g of sand before the start of each trial. For the recording device,a phone (S10+) with slow motion feature capable of recording at 480fps was installed. It was stabilized and attached to the table using an adjustable phone clamp.

We used 5 funnels of different diameters (D=10.29mm, 11.23mm, 12.74mm, 14.49mm, 16.34mm) during the trials that were measured using digital calipers at their bottom tubes. Since the counterweight is heavier than the bucket, it was rested on the surface of the table at the beginning of each trial, so that the system would only start its motion once the bucket had accumulated enough mass to overcome the weight of the counterweight. It was also ensured that the string was rested inside the grooves of the pulleys before each trial to prevent any added friction to the system. Sand was then loaded into the funnel with its aperture covered by a finger to prevent sand from leaking into the bucket before the start of the trial. This was the only method available that would eliminate any additional forces applied to the funnel that could potentially perturb the flow rate of sand. The cell phone was put on recording mode when the finger was removed so that sand was able to flow into the bucket. To prevent the direct impact of the bucket and the table, the bucket was manually caught before its contact. Simultaneously, the start button in Vernier Graphical Analysis, which is the computer software that records the measurements from the dual range force sensor (Vernier), was initiated to start taking measurements until the end of the bucket's motion.

4 Theory

Since our experiment consists of many moving components that revolve around the changes in velocities and masses, basing our theoretical model on the concept of momentum is best. Momentum is a vector quantity denoted as $\vec{\mathbf{p}}$ and is mathematically defined as (LibreTexts):

$$\vec{\mathbf{p}} = m\vec{\mathbf{v}} \tag{1}$$

where m is the mass of the object that is travelling at the velocity $\vec{\mathbf{v}}$. When there is a change in momentum, there must be a net force acting on the body (LibreTexts), this is given in the vector equation:

$$\vec{\mathbf{F}}_{net} = \frac{d\vec{\mathbf{p}}}{dt} \tag{2}$$

Since the sand is falling into the bucket and that the entire Atwood system is moving with the same acceleration, we only analyze the motion of the bucket, basing on the assumption that the tension in the string remains constant, or the string does not stretch. We start by identifying the forces in the free body diagram as shown in Figure 3. There are three forces acting on the bucket: the first is

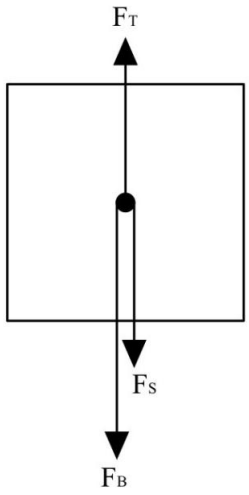

Figure 3: Free body diagram of the bucket

the gravitational force of the bucket F_B, which includes the mass of the bucket and the mass of any added sand; the force of sand F_S, caused by a column of sand exerting a force on the bucket; and the tension F_T due to the string. Since the bucket and sand are falling simultaneously, we must look at the case of a column of sand falling as shown in Fig. 4 to determine the force exerted by the sand:

For the case of a static bucket: the mass accumulated by the falling sand at time $t + dt$ is equivalent to that of $m(t + dt)$; however, since the sand is falling at a velocity relative to that of the bucket, $m(t + dt)$, the mass must be adjusted for the sand that does not make it to the bucket at that time as we assume that the bucket is falling at a higher velocity than the sand. In Figure 4, the highlighted column of sand is the assumed amount of sand that does not make it to the bucket, which we denote as a differential quantity of mass dm', defined according to the parameters:

$$dm' = \rho_s A h \tag{3}$$

Where A is the cross sectional area of the sand column, ρ_s is the density of the sand and h is the height of the sand column. Since the height of the sand column can be found using the speed of the sand, where $h = v_s dt$. Under the assumption that v_s is constant, the cross sectional area of the column of sand is dependent on the diameter of the aperture of the funnel, $A = \pi r^2$, we can substitute these parameters into Eq. 3:

$$dm' = \rho_s \pi \left(\frac{D}{2}\right)^2 v_s dt$$

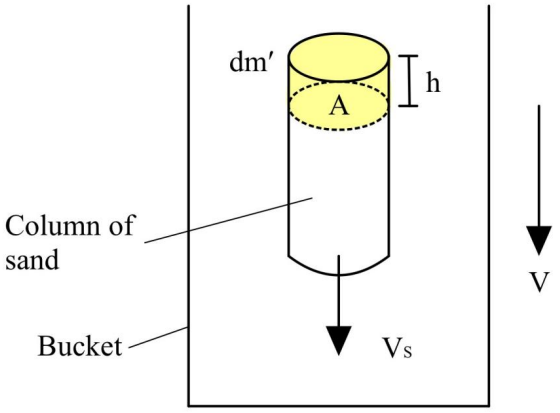

Figure 4: Diagram of a column of sand falling at some time $t + dt$, where the differential mass dm' does not make it to the bucket

As the experimental data will later suggest in Section.5 , sand flows through the aperture at a constant rate, which we denote as c, giving us: $\frac{dm}{dt} = c$. Therefore, the mass dM that flows into the bucket adjusted for those that do not make it can be expressed as:

$$\begin{aligned} dM &= cdt - \rho_s \pi \left(\frac{D}{2}\right)^2 v_s dt \\ &= \left(c - \rho_s \pi \left(\frac{D}{2}\right)^2 v_s\right) dt \end{aligned}$$

For simplification, we call the constant term multiplying dt as k, and integrating this expression gives us:

$$M(t) = kt \tag{4}$$

With the mass as a function of time, we can compute the the force exerted by the jet of sand using the velocity of the sand relative to that of the bucket (or system), which we express $v'(t) = v_s - v$, where v is the velocity of the bucket. Substituting into Eq. 2 gives us,

$$F_S = \frac{d(Mv')}{dt}$$

Since both parameters inside the differentiation operator are functions of time, we can use the product rule to get,

$$F_S = M\frac{dv'}{dt} + v'\frac{dM}{dt} \tag{5}$$

The other forces acting on the bucket are much easier to compute. Starting with the gravitational force:

$$F_B = (M + m_B)g \tag{6}$$

Where m_B is the mass of just the bucket without any added sand. The tension in the string can be computed from a free body diagram of the counterweight, as they are both moving at the same acceleration as shown in Figure 5,

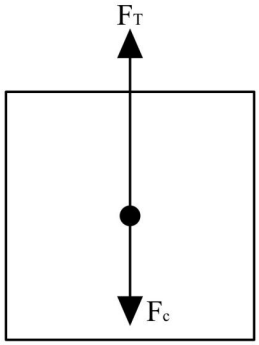

Figure 5: Free body diagram of the counterweight

The net force on the counterweight is:

$$F_T - F_c = m_c a$$
$$F_T = m_c \frac{dv}{dt} + m_c g$$

Simplifying this expression gives us,

$$F_T = m_c \left(\frac{dv}{dt} + g \right) \tag{7}$$

We can now write the net force on the bucket based on the free body diagram from Figure 3 :

$$F_{net} = F_S + F_B - F_T \tag{8}$$

Substituting Eq. 5, Eq. 6 and Eq. 7 in the above gives us:

$$F_{net} = M \frac{dv'}{dt} + v' \frac{dM}{dt} + (M + m_B)g - m_c \left(\frac{dv}{dt} + g \right)$$

Writing the net force in terms of the rate of change of velocity with respect to time and substituting $v' = v_s - v$ gives us:

$$(M + m_B)\frac{dv}{dt} = M \frac{d(v_s - v)}{dt} + (v_s - v)\frac{dM}{dt} + (M + m_B)g - m_c \left(\frac{dv}{dt} + g \right)$$
$$(M + m_B + m_c)\frac{dv}{dt} = M \frac{dv_s}{dt} - M \frac{dv}{dt} + (v_s - v)\frac{dM}{dt} + (M + m_B - m_c)g$$

Here, since we identify the term $\frac{dM}{dt}$ as the constant k in Eq. 4, we can further simplify our expression as,

$$(2M + m_B + m_c)\frac{dv}{dt} = M \frac{dv_s}{dt} + (v_s - v)k + (M + m_B - m_c)g$$
$$(2M + m_B + m_c)\frac{dv}{dt} + vk = M \frac{dv_s}{dt} + (M + m_B - m_c)g + v_s k$$

We will make the assumption that gravity is the only force acting on the sand, meaning that its velocity v_s can be expressed as $v_s = gt$. Applying this along with the derived M in Eq. 4, where $M = kt$, we can simplify as follows,

$$(2kt + m_B + m_c)\frac{dv}{dt} + vk = (3kt + m_B - m_c)g$$

This non-homogeneous differential equation of the first order can be solved for the function $v(t)$ by integrating using an integration factor $\mu(t)$. We can multiply the entire expression by $\mu(t)$:

$$\mu(t)\frac{dv}{dt} + \mu(t)\frac{k}{2kt + m_B + m_c}v = \mu(t)\left(\frac{(3kt + m_B - m_c)g}{2kt + m_B + m_c}\right)$$

The integration factor has the property that $\mu(t)p(t) = \frac{d\mu}{dt}$. In this case, we have,

$$p(t) = \frac{k}{2kt + m_B + m_c}$$

To avoid carrying out these complicated expressions, we have assigned the term on the RHS as $q(t)$,

$$q(t) = \frac{(3kt + m_B - m_c)g}{2kt + m_B + m_c}$$

This simplifies the expression to,

$$\mu(t)\frac{dv}{dt} + v\frac{d\mu}{dt} = q(t)\mu(t)$$

Since the LHS is identified as the result of a product rule, we can simplify it to $\frac{d}{dt}(\mu(t)v(t))$ and integrate both sides with respect to dt,

$$\int \frac{d}{dt}(\mu(t)v(t))dt = \int q(t)\mu(t)dt$$

Upon simplifying, we get,

$$v(t) = \frac{\int q(t)\mu(t)dt}{\mu(t)} \tag{9}$$

From this point, we must compute the integral and determine the expression for the integration factor. The integration factor is:

$$\mu(t) = e^{\int p(t)dt}$$

We can substitute our $p(t)$ into the above expression,

$$\mu(t) = \exp\left(\int \frac{k}{2kt + m_B + m_c}dt\right)$$

Evaluating the integral gives us,

$$\begin{aligned}\mu(t) &= \exp\left(\frac{1}{2}\ln(2kt + m_B + m_c) + C_1\right) \\ &= \mu_0\sqrt{2kt + m_B + m_c}\end{aligned}$$

where $\mu_0 = e^{C_1}$ is an unknown constant as a result of the integration constant. We can substitute the integration constant and the simplified expression of $q(t)$ into the integral in Eq. 9 to get,

$$\begin{aligned}\int q(t)\mu(t)dt &= \mu_0\int \frac{(3kt + m_B - m_c)g}{2kt + m_B + m_c}\sqrt{2kt + m_B + m_c}dt \\ &= \mu_0\int \frac{(3kt + m_B - m_c)g}{\sqrt{2kt + m_B + m_c}}dt\end{aligned}$$

The detailed evaluation of this integral will not be included but using integration by substitution results in:

$$\int q(t)\mu(t)dt = \frac{\mu_0 g\sqrt{2kt + m_B + m_c}(kt - 2m_c)}{k} + C_2 \tag{10}$$

where C is the integration constant again. We can finally substitute Eq. 10 along with the integration factor into our expression for $v(t)$ of Eq. 9. Simplifying that expression gives us the final,

$$v(t) = gt - \frac{2gm_c}{k} + \frac{C_2}{\sqrt{2kt + m_B + m_c}} \tag{11}$$

We can solve for the integration constant given the initial condition of our system. Since at $t = 0$, our system remains static until it gains enough mass to outweigh the counterweight as we recall that $m_B < m_c$ initially. This signifies that the velocity $v = 0$ at time $t = 0$, giving us enough information to solve for the constant, which turns out to be:

$$C_2 = \frac{2gm_c\sqrt{m_B + m_c}}{k}$$

Substituting the constant gives us the final $v(t)$ function:

$$v(t) = -gt - \frac{2gm_c}{k}\left(\frac{\sqrt{m_B + m_c}}{\sqrt{2kt + m_B + m_c}} - 1\right) \tag{12}$$

With the velocity function, we can get the function of height by simply integrating Eq. 12,

$$h(t) = C - \frac{gt^2}{2} - \frac{2gm_c}{k^2}\left(\sqrt{(m_B + m_c)(2kt + m_B + m_c)} - kt\right)$$

At time $t = 0$, our system is at a height h_0. As a result, the integration constant becomes,

$$C_2 = h_0 + \frac{2gm_c}{k^2}(m_B + m_c)$$

Finally we substitute the integration constant back into our expression of $h(t)$ to get the height of the bucket as a function of time:

$$h(t) = h_0 - \frac{gt^2}{2} - \frac{2m_cg}{k^2}\left(\sqrt{(2kt + m_B + m_c)(m_B + m_c)} - (m_B + m_c + kt)\right) \tag{13}$$

Eq. 13 tells us about how the height of the bucket changes during its falling motion, and can be applied to the experimental results through curve fitting to verify the validity of our experimental results.

5 Results and Analysis

The videos recorded in Section 3 were loaded into Tracker, which is a video analysis software that allows the motion of objects to be analyzed (Tracker). A screenshot of the Tracker interface is shown in Figure 6. The frame rate of the footage was set to 480fps, and the "calibration stick" in tracker was assigned a length of 20cm. The purpose of a calibration stick is to adjust the video scale with the real scale of the captured objects. By processing the videos on Tracker, we were able to obtain the bucket's height as a function of time. We noticed that the bucket's motion consisted of two phases, which can be seen in Figure 7.

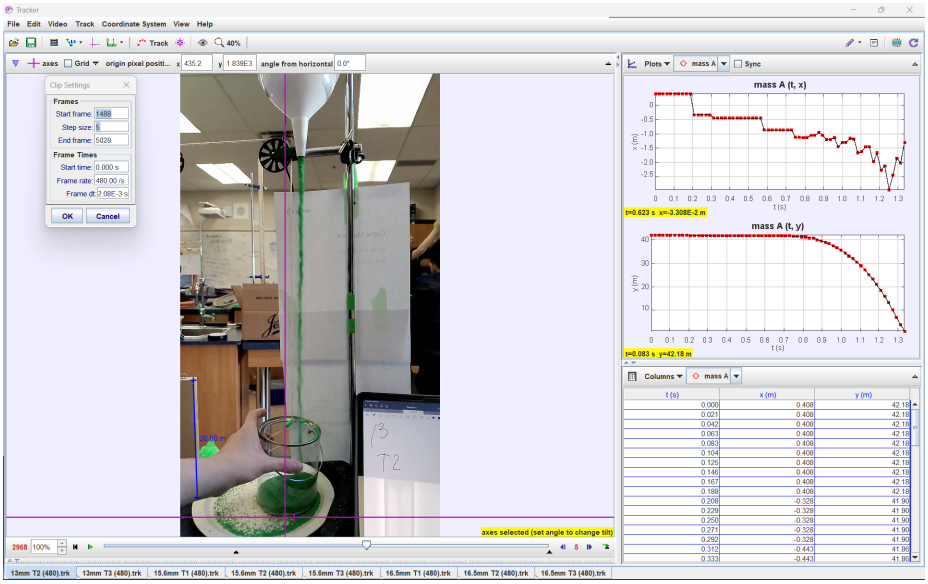

Figure 6: Tracker interface to track how the bucket's height varies over time

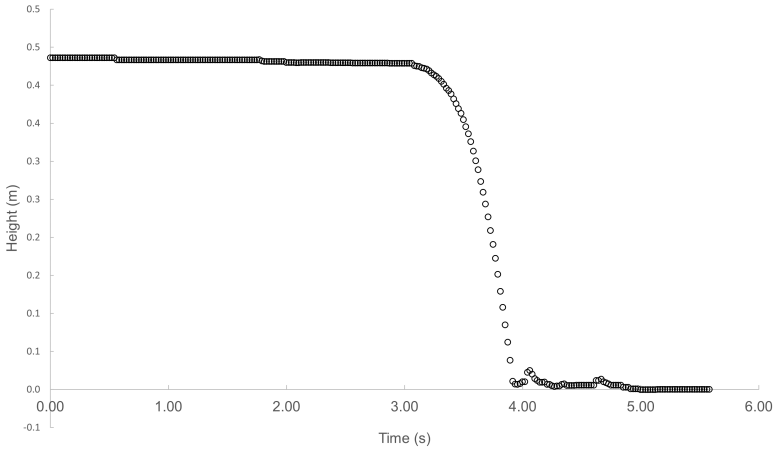

Figure 7: Motion of the bucket that consists of two phases: mass gaining phase and falling phase

The first phase is the bucket gaining mass to overcome the weight difference between the bucket and counterweight, which is 43.3g; the second phase is the falling phase of the bucket after it overcame the friction in the pulley. The theoretical model in Eq. 13 is only applicable for the falling phase as the height of the bucket only starts to change when the bucket has accumulated enough mass to overcome the weight of the counterweight. To see whether our theoretical model agrees with the experimental results, we fitted Eq. 13 to the falling phase of each trial, which can be seen in Figure 8.

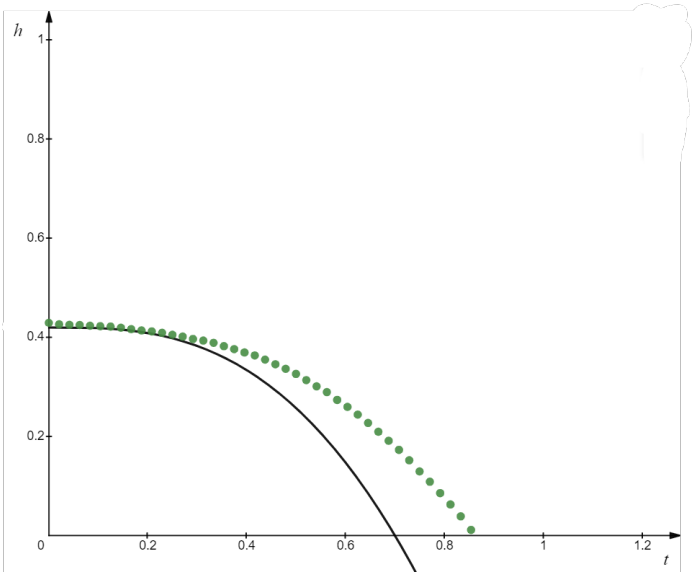

Figure 8: Curve fitting Eq. 13 to the experimental results of height as a function of time.

The model in Figure 8 reflects the experimental results at the earlier stages of falling, but starts to deviate more and more at later times. As we are attempting to find the total falling time of the bucket, which includes the gain mass time, by graphing the height as a function of time, Eq. 13, on Desmos and finding its corresponding x coordinate of the x-intercept, we are able to obtain the theoretical time it takes for the falling phase. For the gaining mass phase, we need to look at the results from the vernier force sensor, where it produces a force as a function of time graph of the funnel. Under the assumption that the rate of weight loss of the funnel is the same as the weight gain of the bucket, we can get mass as a function of time by dividing the measured force values by gravitational field strength: 9.81 m/s^2. This results in mass as a function of time, and the averaged values of the flow rates of the first aperture diameter, 10.29mm is seen in Figure 9,

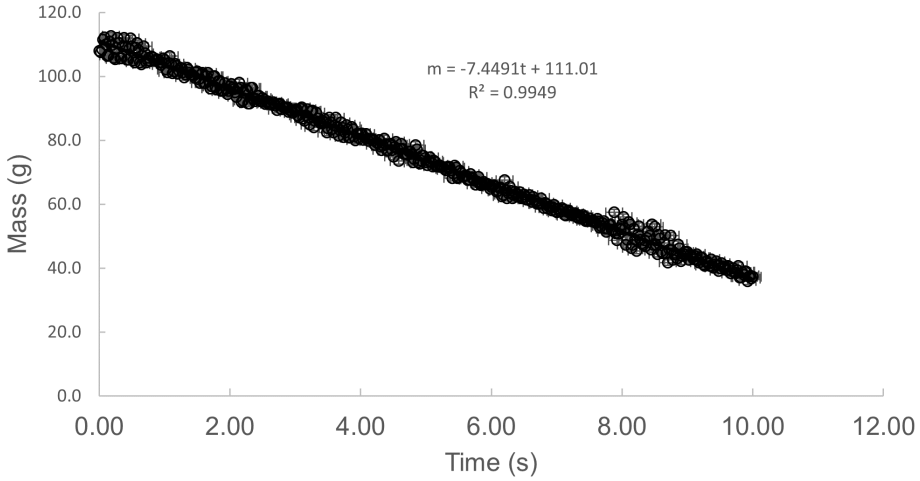

Figure 9: The mass of the funnel as a function of time of the smallest aperture diameter: 10.29mm

Figure 9 shows a strong linear correlation between the mass of the funnel and time, with a R^2 value of 0.9949. The slope of the graph is the rate of change of mass over time, which is the flow rate in g/s. We use this these equations of best fit lines to predict the time it takes for the bucket to gain enough mass such that the mass of the bucket is the same as the counterweight, $m_B = m_c$ before it

starts moving. The computed values can be seen in Table 1,

Table 1: Measured and calculated values of flow rates, mass gain time, falling time and total time of different aperture diameters

Aperture Diameter (± 0.01mm)	Mass gain time (± 0.002s)	Falling time (± 0.002s)	Total time (± 0.004s)	Flow rate (g\s)
10.29	3.121	0.916	4.037	7.4 ± 0.2
11.23	1.222	0.701	1.923	17.9 ± 0.4
12.74	0.736	0.621	1.257	28.5 ±0.3
14.49	0.464	0.483	0.947	50.4 ± 0.6
16.34	0.400	0.411	0.811	63.5 ± 0.1

Table 1 presents the calculated and measured values of flow rates, mass gain time, falling time and total time in relation to the aperture diameter of the funnels. We can plot the total falling time of the bucket against the aperture diameter as shown in Figure 10.

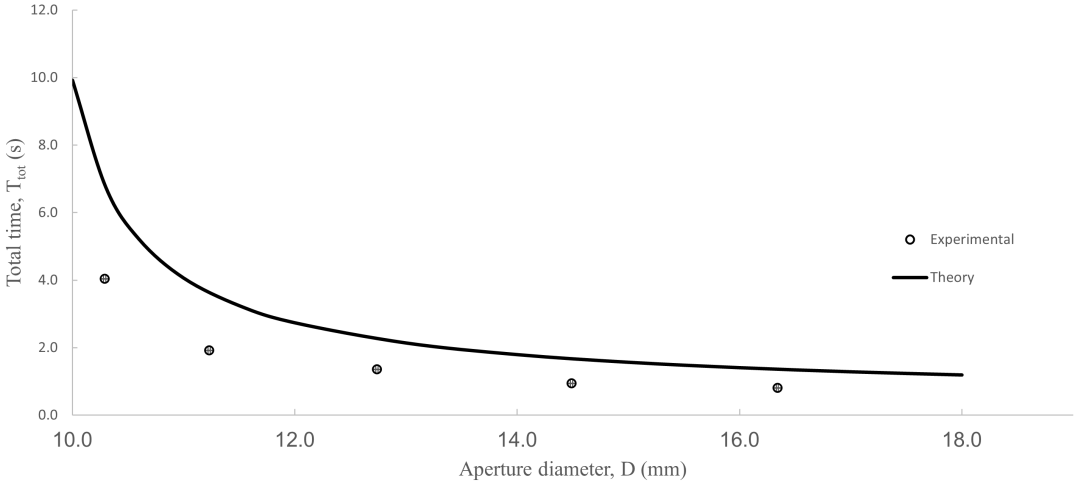

Figure 10: The effects of aperture diameter on the total falling time

Figure 10 shows the relationship between aperture diameters of the funnels with the total time of the bucket's motion. We computed the theoretical model based on the two phases mentioned previously, where the mass gain time over a number of aperture diameters is given by $t = \frac{m_{diff}}{c}$, where m_{diff} is the mass difference between the counterweight and the mass of the bucket, and c is the flow rate of a particular aperture diameter. Since we do not have any models that relate flow rate with aperture diameter, we computed the flow rates by interpolating and extrapolating values from a graph of flow rate against aperture diameter as shown in Figure 11.

Using Figure 11, we computed the mass gain time associated with a series of aperture diameters. These values were combined with the falling times, which were computed by graphing Eq. 13 and finding the x-intercepts associated with the flow rates, which are the times it takes for the bucket to fall from its initial height to $h = 0$. From Figure 10, we noticed that as aperture diameters increase, the total falling time decreases, which agrees with how when the aperture diameter increases, the flow rate increases and therefore decreasing the time it takes to gain the mass difference. This ultimately combines with the decreased falling time, as the force exerted by the sand on the bucket increases due to more sand flowing out of the bucket, to decrease the total falling time of the bucket. We also noticed that the experimental values are consistently lower than the theoretical curve, and we explore the possible explanations further in Section 6.

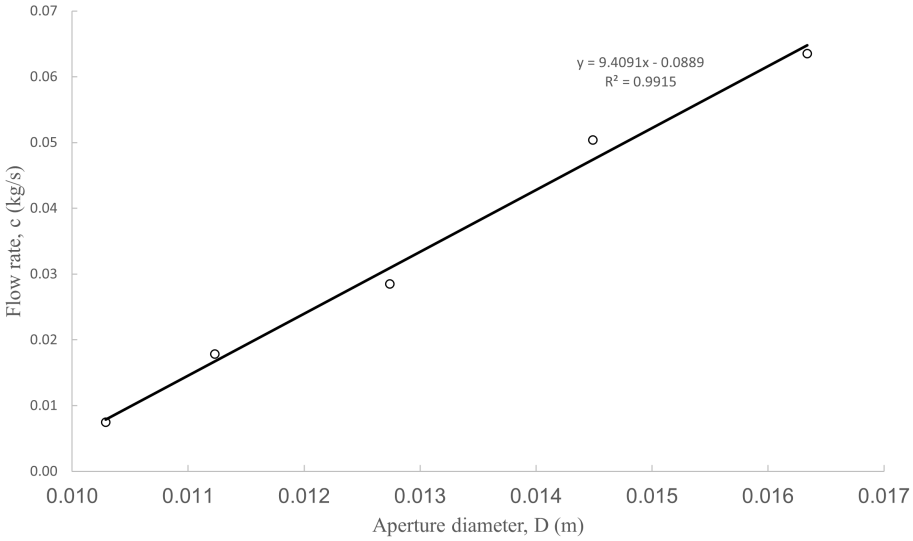

Figure 11: Relationship between flow rate and aperture diameter of the funnel

6 Evaluation and Conclusion

In this investigation, we explored the relationship between aperture diameter and the total falling time of a variable mass Atwood machine. The experimental results in Figure 10 suggests a systematic deviation from our theoretical model - there are a few possible explanations for this phenomenon. During the experiment, it was noticed that the column of sand does not land in the middle of the bucket, instead, over a period of time, sand entering the bucket would pile up in a corner, causing the bucket to tilt relative to the pivot point of the bucket that is hanging by the string. This effectively increases the distance between the pivot point to the pile of sand, and as the concept of torque suggests, increased distance from the pivot point implies an increase in torque, and thus greater angular acceleration. This could be a potential explanation to the significant deviation in the total time (see Figure 10) as greater angular acceleration means a higher linear velocity. This ultimately led to the bucket being able to overcome the weight difference given by the counterweight, and lowering the total time systematically in all trials. One way to minimize the effect of this problem is to ensure that the funnel tube is directly placed on top of the middle of the bucket, so that the sand would not pile up in a corner. Another explanation could be due to the errors in the force sensor measurements as it has an uncertainty of ± 0.1N (Vernier), which leads to an approximate error of ± 10g in the mass flow rate. As we obtain the flow rates of the different apertures through linear approximation, there must be an error in the associated slope as there are errors in the measurements. We computed the maximum and minimum slopes and the associated errors in the flow rates are given by the range uncertainty of the two maximum and minimum slopes. However, the effects of the errors in the force sensor are not significant enough to explain the deviation in Figure 10. Another possible explanation could be the added momentum due to the falling sand from the funnel to the bucket during the mass gain phase. Since the sand falls from a certain height, it carries a certain momentum with it when coming in contact with the bucket. Therefore, the collision between the sand particles and the bucket results in the bucket having a greater velocity by conservation of momentum. This could be a potential explanation for the significantly less time in the mass gain phase in our experimental results in comparison with our model, which did not include added momentum.

In this experiment, we used sand as the source of granular flow for the mass gain of the bucket. However, since we did not know whether the height of the sand inside the funnel will have a significant impact on its flow rate, we can extend this investigation to using fluids, where the effect of height on flow rate can be explored using Bernoulli's equation.

Works Cited

Admin. “Atwood Machine - Definition, Formula, Calculation, Uses, Faqs.” *BYJUS*, BYJU'S, 14 June 2022, https://byjus.com/physics/atwood-machine/.

“Dual-Range Force Sensor.” *Vernier*, https://www.vernier.com/product/dual-range-force-sensor/.

Libretexts. “5.4: Newton's Second Law.” *Physics LibreTexts*, Libretexts, 12 Sept. 2022, https://phys.libretexts.org/Bookshelves/University_Physics/Book%3A_University_Physics_(OpenStax)/Book%3A_University_Physics_I_-_Mechanics_Sound_Oscillations_and_Waves_(OpenStax)/05%3A_Newton%27s_Laws_of_Motion/5.04%3A_Newton%27s_Second_Law.

“Try Tracker Online.” *Tracker Video Analysis and Modeling Tool for Physics Education*, https://physlets.org/tracker/.